

## Bound states of the two-roton Schrodinger equation

This article has been downloaded from IOPscience. Please scroll down to see the full text article.

1974 J. Phys. A: Math. Nucl. Gen. 7 1283

(<http://iopscience.iop.org/0301-0015/7/11/008>)

View [the table of contents for this issue](#), or go to the [journal homepage](#) for more

Download details:

IP Address: 171.66.16.87

The article was downloaded on 02/06/2010 at 04:51

Please note that [terms and conditions apply](#).

## Bound states of the two-roton Schrödinger equation

Paul H Roberts† and William J Pardee‡

Department of Physics, University of Oregon, Eugene, Oregon 97403, USA

Received 28 December 1973, in final form 6 March 1974

**Abstract.** Bound states of two rotons are sought by explicit numerical integration of a Schrödinger equation, based on an interaction hamiltonian of dipole-dipole form and self-hamiltonians derived from the modified Landau dispersion relationship. It is found that the most tightly bound state of zero total momentum belongs to the angular momentum quantum number  $l = 3$ . The binding energy is about 0.43 K, and the root mean square separation of the rotons is almost 12 Å. Bound states for other values of  $l$  are located. In particular, the greatest binding energy of the  $l = 2$  bound state is about 0.29 K, in satisfactory agreement with the experimentally determined value of  $(0.37 \pm 0.10)$  K with a root mean square roton separation of just over 14 Å. The largest effective masses of these  $l = 2$  and  $l = 3$  states are respectively about 2.1 and 2.8 times the mass of the helium atom.

### 1. Introduction

Raman scattering of optical photons by liquid helium has suggested the existence of a loosely bound state of two rotons (Greytak and Yau 1969, Greytak *et al* 1970). Depolarization data indicate that the angular momentum  $l = 2$  is preferred, although other values may be present as well (Greytak and Yau 1969). We find below bound states of the Schrödinger-like equation following from the roton dispersion curve and the hydrodynamic interaction between two widely separated rotons. We solve the equation for zero centre of mass momentum  $P$ , and then treat non-zero  $P$  by first-order perturbation theory. We find a series of excitation curves, measurable in principle via neutron scattering, of the form

$$E(P) = 2\Delta - E_l + P^2/(2M^*). \quad (1)$$

For each energy eigenvalue  $E_l$  there are  $l + 1$  effective masses,  $M^*$ , labelled by the internal quantum number  $m = |L_z|$ . In (1),  $\Delta$  denotes the roton energy gap.

The idea of two distinct rotons interacting via a potential can be sensible only if we restrict ourselves to He II excitations which are localized wave packets with momentum distribution peaked around some value near the roton minimum. The flow at a point  $r_1$ , situated at a large distance  $r$  from a roton of momentum  $p_2$  at  $r_2$ , is (Feynman and Cohen 1956, Feenberg 1969)

$$V_s(r) = \frac{1}{4\pi\rho} \left( \frac{3(p_2 \cdot r)r}{r^5} - \frac{p_2}{r^3} \right), \quad (2)$$

† Permanent address: School of Mathematics, University of Newcastle upon Tyne, UK.

‡ Now at Department of Physics, Indiana University, USA.

where  $\rho$  is the fluid density. The energy of a roton of momentum  $\mathbf{p}_1$  situated at  $\mathbf{r}_1$  in this flow is

$$E_1 = \epsilon(\mathbf{p}_1) + \mathbf{p}_1 \cdot \mathbf{V}_s(\mathbf{r}). \quad (3)$$

The hamiltonian of the system is then

$$H(\mathbf{p}_1, \mathbf{p}_2, \mathbf{r}) = \epsilon(\mathbf{p}_1) + \epsilon(\mathbf{p}_2) + \mathbf{p}_1 \cdot \mathbf{V}_s(\mathbf{r}), \quad (4)$$

which, despite its appearance, is symmetric in the variables of the two rotons. Although this interaction is semi-classical and reasonable only for rather large separations, one notes that experiments suggest the average separation is large: if  $\mu$  denotes the effective mass of the roton, and  $E_2$  is the experimentally determined binding energy of 0.37 K, then  $\hbar/(\mu E_2)^{1/2}$  is about 14.3 Å. Moreover, the angular momentum barrier present for  $l \geq 2$  may be expected to reduce sensitivity to the unknown short-distance behaviour of the potential.

The conventional (Landau) form for  $\epsilon(\mathbf{p})$  is

$$\epsilon(\mathbf{p}) = \Delta + (|\mathbf{p}| - p_0)^2 / (2\mu), \quad (5)$$

where  $p_0$  is the momentum corresponding to the roton minimum. It should be recalled, however, that a Schrödinger equation is to be formed from the hamiltonian (4), and for this purpose the form (5) is both ambiguous and unsuitable. Again remembering that the binding energy is very small, we can expect contributions only from  $(|\mathbf{p}| - p_0)^2 \ll p_0^2$ . This suggests that we should replace the spectrum (5) by the more convenient modified Landau form apparently first introduced by Pitaevski, and used for example by Iguichi (1971):

$$\epsilon(\mathbf{p}) = \Delta + (p^2 - p_0^2)^2 / (8\mu p_0^2). \quad (6)$$

The location and curvature of this dispersion curve coincide with those of equation (5). Indeed, equation (6) is a distinctly better fit to the data† than is the conventional expression (see figure 1). Thus, after absorbing  $2\Delta$  into the zero of energy, we have for our hamiltonian

$$H(\mathbf{p}_1, \mathbf{p}_2, \mathbf{r}) = \frac{(p_1^2 - p_0^2)^2}{8\mu p_0^2} + \frac{(p_2^2 - p_0^2)^2}{8\mu p_0^2} + \frac{1}{4\pi\rho} \left( \frac{3(\mathbf{p}_1 \cdot \mathbf{r})(\mathbf{p}_2 \cdot \mathbf{r})}{r^5} - \frac{\mathbf{p}_1 \cdot \mathbf{p}_2}{r^3} \right). \quad (7)$$

If the total momentum  $\mathbf{p}_1 + \mathbf{p}_2$  is zero, the hamiltonian (7) gives stable bound orbits in classical mechanics, but with a binding energy more than an order of magnitude too large. We find that a quantum-mechanical bound state exists for  $l = 2$ , which has approximately the experimental energy. An  $l = 3$  bound state also exists having a slightly greater binding energy, as well as numerous other weakly bound states. We wish to emphasize that the present approach, unlike that of Yau and Stephen (1971), is not variational but depends on a direct integration of the Schrödinger equation. Also our results do not rely on the arbitrary introduction of a small  $r$  cut-off,  $R_c$ , specially selected to agree with the experimental results best.

## 2. Formulation and solution of the eigenvalue problem

The relative coordinate  $\mathbf{r} = \mathbf{r}_1 - \mathbf{r}_2$  is conjugate to the relative momentum operator  $\mathbf{p} = \frac{1}{2}(\mathbf{p}_1 - \mathbf{p}_2)$  satisfying  $[r_i, p_m] = i\hbar\delta_{im}$ . For small total momentum  $\mathbf{P} = \mathbf{p}_1 + \mathbf{p}_2$  we

† A convenient and thorough analysis of the data has recently been given by Brooks and Donnelly (1974).

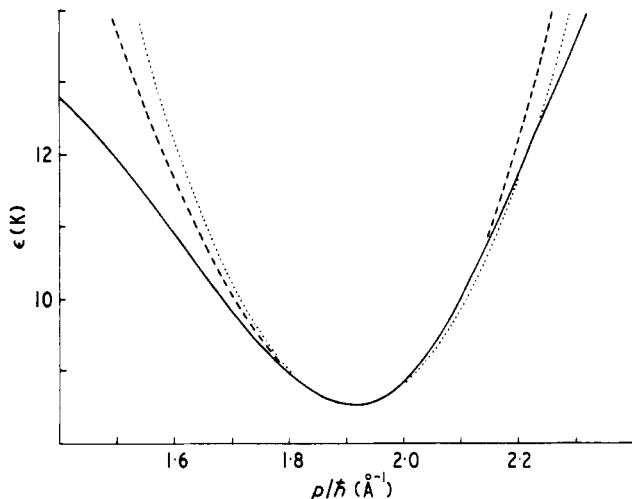


**Figure 1.** A comparison of the dispersion relationship with two approximations. The full curve gives the actual spectrum of quasi-particles, as given by a six-term series fitting of observational data at  $T = 1.1$  K and the vapour pressure (Brooks and Donnelly 1974). The parameters for the roton minimum are  $\Delta = 8.5458$  K,  $p_0/\hbar = 1.9128$  Å<sup>-1</sup>, and  $\mu = 0.15967 m_{\text{He}}$ . The dotted curve shows the Landau spectrum and the broken curve shows the modified Landau spectrum implied by these parameters.

can, with  $O(P^4)$  error, write  $H = H_0 + H_1$ , where

$$H_0 = \frac{1}{2}(p^2 - 1)^2 - V_{ij}p_i p_j, \quad (8)$$

$$H_1 = \frac{1}{4}(\mathbf{P} \cdot \mathbf{p})^2 + \frac{1}{2}P^2(p^2 - 1) + V_{ij}P_i P_j, \quad (9)$$

$$V_{ij} = \frac{1}{2} \left( \frac{3r_i r_j}{r^5} - \frac{\delta_{ij}}{r^3} \right), \quad (10)$$

and summation over repeated indices is understood. We have used dimensionless units based on  $\lambda = (2\pi\rho/\mu)^{-1/3}$  for length,  $p_0$  for momentum, and  $p_0^2/\mu$  for energy. Denoting the dimensionless parameter  $\hbar/(\lambda p_0)$  ( $=0.499$ ) by  $\sigma$ , and replacing the dimensionless  $\mathbf{p}$  by  $-\mathbf{i}\sigma\nabla$ , the Schrödinger equation  $(H_0 - E)\Psi = 0$  for the states of zero total momentum becomes

$$\sigma^4 \nabla^4 \Psi + 2(1 - r^{-3})\sigma^2 \nabla^2 \Psi + 6\sigma^2 r^{-3} \frac{\partial^2 \Psi}{\partial r^2} = (4E - 1)\Psi. \quad (11)$$

The hermiticity condition  $(\Phi, H_0 \Psi) = (\Psi, H_0 \Phi)$  requires that

$$r^2 \sigma^2 \left( \Phi \frac{\partial}{\partial r} \nabla^2 \Psi - \frac{\partial \Phi}{\partial r} \nabla^2 \Psi + \frac{\partial \Psi}{\partial r} \nabla^2 \Phi - \Psi \frac{\partial}{\partial r} \nabla^2 \Phi \right) + 2r^2(1 + 2r^{-3}) \left( \Phi \frac{\partial \Psi}{\partial r} - \Psi \frac{\partial \Phi}{\partial r} \right) \quad (12)$$

should vanish for  $r \rightarrow 0$  and for  $r \rightarrow \infty$ . These conditions transform (11) into an eigenvalue problem, as we shall see.

Equation (11) admits separable solutions of the form  $\Psi = R(r)Y_{lm}(\theta, \phi)$ , where  $Y_{lm}$  is a spherical harmonic of order  $l$ . We will examine only the cases  $l \geq 2$ . It can be shown that as  $r \rightarrow \infty$ ,  $R$  approaches a linear combination of  $r^{-1} \exp(q_i r)$ , where  $\sigma q_i$  takes the four values

$$\sigma q = \pm [(\frac{1}{4} - E)^{1/2} - \frac{1}{2}]^{1/2} \pm i[(\frac{1}{4} - E)^{1/2} + \frac{1}{2}]^{1/2}. \quad (13)$$

Condition (12) requires that only the two values of  $q$  with negative real part appear in the eigensolution. This places essentially two conditions on the solutions of the fourth-order equation (11).

Analysis of the solutions of (11) for  $r \rightarrow 0$  reveals two types of behaviour. The solutions which we will call 'regular' are characterized by a small  $r$  asymptotic behaviour of the form  $\Psi \sim r \exp(\pm i s \ln r)$ , where  $s^2 = \frac{1}{2}l(l+1) - 1$ . The 'irregular' solutions are asymptotically given by  $\Psi \sim r^{5/4} \exp[\pm 4i/(\sigma r^{1/2})]$ . Condition (12) permits only regular solutions in an eigenfunction. This provides two further conditions on the fourth-order equation (11), thus completing the definition of the eigenvalue problem. We will call this the 'coreless model', to distinguish it from the next two possibilities.

The dipole interaction is quite unrealistic for small  $r$ , and even the idea of two distinct rotors is questionable. One might place a potential barrier  $V = V_c$  at  $r = R_c$  to represent a hard-core repulsion. The requirement of continuity of  $R$  and its first three derivatives at  $r = R_c$  becomes, as  $V_c \rightarrow \infty$ , the condition that  $R$  and  $dR/dr$  vanish at  $r = R_c$ . These two demands, together with the two on  $R$  at infinity, also pose a well defined eigenvalue problem which we may call the 'hard-core model'. Another extreme possibility would be to set  $V = 0$  for  $r < R_c$ , and to exclude the two spherical Bessel functions (of the four which satisfy the differential equation for  $r < R_c$ ) which diverge at the origin. This defines a 'soft-core model'.

One of the difficulties in solving equation (11) is a consequence of the small size of the eigenvalue  $E_l$ . This implies that the real part of  $q$  is small in modulus and that the numerical integrations must be carried to large  $r$  before the solution can be properly tested for the absence of exponentially growing components. To overcome this difficulty, the terms in the asymptotic expansion of  $R$  for  $r \rightarrow \infty$  were obtained from equation (11) by a five-term recurrence relation. The Runge-Kutta integration could then be terminated at any  $r (= r_1, \text{ say})$ , and, with the error implied by the asymptotic expansion, extrapolated to infinite  $r$ . The integration of the coreless model also fails as  $r$  approaches zero. This difficulty was overcome in like fashion. An asymptotic expansion of the regular solution was generated by use of a six-term relation and was matched to the Runge-Kutta integration at  $r = r_2$ , say. The accuracy of the results was tested by comparing answers for different choices of  $r_1$  and  $r_2$ .

Once the eigenvalues and eigenfunctions had been obtained, it was straightforward to treat the effect of centre of mass motion in first-order perturbation theory. With the  $z$  axis defined by the direction of  $\mathbf{P}$ , we have

$$\begin{aligned} & \int \Psi^* H_1 \Psi \, dV \\ &= \frac{P^2}{2M^*} \int \Psi^* \Psi \, dV = \frac{P^2}{8} \left( \frac{2(l^2 + l - 3m^2)}{(2l-1)(2l+3)} \int \frac{|\Psi|^2}{r^3} \, dV \right. \\ & \quad \left. + \sigma^2 \frac{(8l^2 + 8l - 5 - 4m^2)}{(2l-1)(2l+3)} \int |\nabla \Psi|^2 \, dV - \int |\Psi|^2 \, dV \right), \end{aligned} \quad (14)$$

where  $m$  is the azimuthal quantum number and  $M^*$  is the effective mass of the bound state in units of the roton mass  $\mu \simeq 0.16 m_{\text{He}}$  where  $m_{\text{He}}$  is the mass of the helium atom. We note that the excitation curves given by expression (1) cross, producing mixing of states of different  $l$  and repulsion of levels. The spectrum obtained here may be, therefore, valid only for very small  $|\mathbf{P}|$  and not be a good approximation to that observed in actual neutron scattering.

### 3. Results and discussion

We consider first the coreless model. The binding energy  $E_l$  of the most tightly bound state (largest  $E_l$ ) is given in table 1 for  $l = 2, 3, 4$  and 5. The upper half of the table summarizes our results in the dimensionless units defined below equation (10) above;

**Table 1.** Binding energy, mean square momentum and effective masses.

$l$	2	3	4	5
$E_l \times 10^3$	1.0520	1.5585	0.3536	0.1086
$\sqrt{\langle p^2 \rangle}$	1.00904	1.00504	1.00118	1.00005
$\sqrt{\langle r^2 \rangle}$	13.58	11.03	21.61	100.1
$M^*(m=0)$	3.679	3.827	3.927	3.965
$M^*(m=1)$	4.484	4.190	4.139	4.104
$M^*(m=2)$	13.04	5.852	4.940	4.587
$M^*(m=3)$	—	17.29	7.288	5.706
$M^*(m=4)$	—	—	21.80	8.664
$M^*(m=5)$	—	—	—	25.98
$E_l(\text{K})$	0.290	0.430	0.0976	0.0300
$\hbar^{-1} \sqrt{\langle p^2 \rangle} (\text{\AA}^{-1})$	1.927	1.920	1.912	1.910
$\sqrt{\langle r^2 \rangle} (\text{\AA})$	14.26	11.59	22.70	105.1
$M^*/m_{\text{He}}(m=0)$	0.5887	0.6123	0.6284	0.6345
$M^*/m_{\text{He}}(m=1)$	0.7175	0.6703	0.6623	0.6567
$M^*/m_{\text{He}}(m=2)$	2.086	0.9364	0.7904	0.7340
$M^*/m_{\text{He}}(m=3)$	—	2.766	1.166	0.9130
$M^*/m_{\text{He}}(m=4)$	—	—	3.488	1.386
$M^*/m_{\text{He}}(m=5)$	—	—	—	4.157

the lower half gives the same results in dimensional form using  $p_0/\hbar = 1.91 \text{ \AA}^{-1}$ ,  $\mu = 0.16 m_{\text{He}}$  and  $\rho = 0.146 \text{ g cm}^{-3}$ . It should be noticed that the lowest energy state appears to belong not to  $l = 2$  but  $l = 3$ . This unexpected result led us to expend considerable computing effort searching for a more tightly bound  $l = 2$  state, but without success. It suggests that the  $l = 3$  bound states will be more highly populated than the  $l = 2$  states observed in Raman scattering experiments. The binding energy for  $l = 2$  is 0.29 K, in satisfactory agreement with the experimentally determined value of  $(0.37 \pm 0.10)$  K. We also calculated  $\langle p^2 \rangle$  and  $\langle r^2 \rangle$ . We found for  $l = 2$  that  $\sqrt{\langle p^2 \rangle}/p_0 = 1.005$ , clearly within the region of validity of the modified Landau spectrum (6). We found the  $l = 2$  root mean square radius  $\langle r^2 \rangle^{1/2}$  to be 14.3 \text{ \AA}, supporting the physical picture described in the introduction. It may be observed that the largest effective mass  $2.1 m_{\text{He}}$  of the  $l = 2$  state is somewhat larger than the estimate of about  $\frac{1}{2} m_{\text{He}}$  made by Donnelly (1972); the classical theory gave  $1.6 m_{\text{He}}$  but for a greater angular momentum than implied by  $l = 2$  (Roberts and Donnelly 1974).

The results of the computations are also shown in figures 2–7. The wavefunction  $R$  is given for  $l = 2$  and 3 in figures 2 and 3. (The abscissa is dimensionless, the normalization of the ordinate is arbitrary.) In figures 4 and 5, the integrated probability  $\mathcal{P}$  is shown for  $l = 2$  and  $l = 3$ , where

$$\mathcal{P}(r) = \int_{v(r)} |\Psi|^2 dV, \quad (15)$$

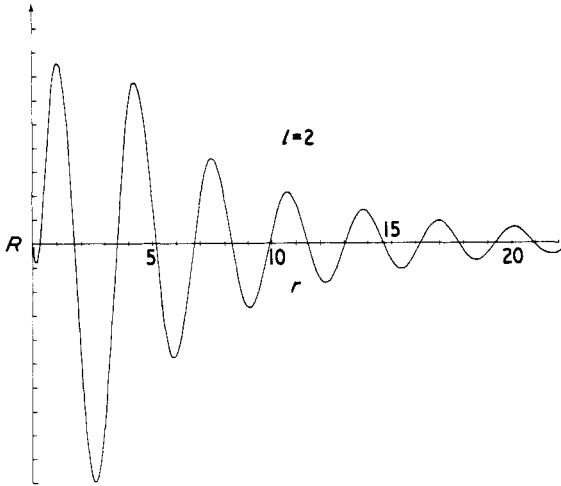


**Figure 2.** The wavefunction  $R$  for  $l = 2$  as a function of dimensionless radius  $r$  in the case of pure dipole-dipole interaction.

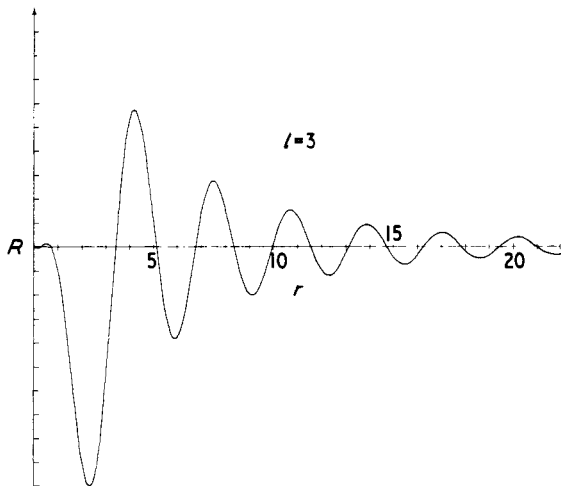


**Figure 3.** The wavefunction  $R$  for  $l = 3$  as a function of dimensionless radius  $r$  in the case of pure dipole-dipole interaction.

$v(r)$  is the interior of the sphere of radius  $r$ , and  $\Psi$  is normalized so that  $\mathcal{P}(\infty) = 1$ . In figure 6 the dispersion curves (1) are given for the results tabulated. In figure 7 the results for  $l = 2$  alone are shown on a diagram which also gives neutron data near  $P = 0$  (Cowley and Woods 1971) and a model dispersion curve (Brooks and Donnelly 1974).

Next, we consider the hard-core model. The dimensionless binding energy  $E_l$  is shown as a function of the dimensionless core radius  $R_c$  in figure 8 for  $l = 2, 3$  and 4. No results were obtained for small values of  $R_c$ , because the presence of the irregular components of solution (necessary to satisfy the boundary conditions at  $r = R_c$ ) can lead to difficulties in the Runge-Kutta integrations for small  $r$ . It is nevertheless clear

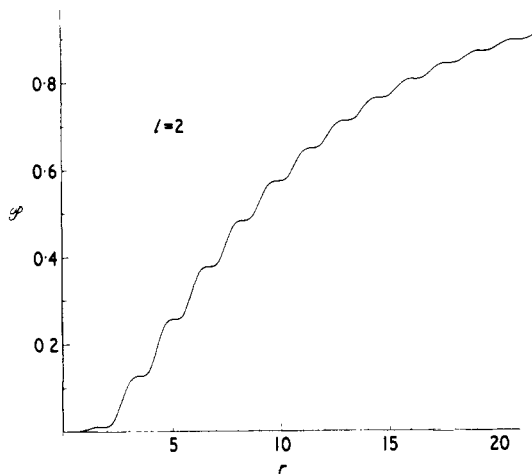


Figure 4. The integrated probability  $\mathcal{P}(r)$  for the wavefunction shown in figure 2;  $\mathcal{P}$  is defined in equation (15), and  $r$  is dimensionless.

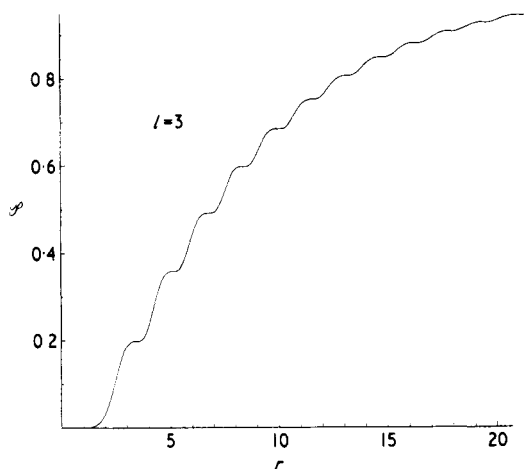


Figure 5. The integrated probability  $\mathcal{P}(r)$  for the wavefunction shown in figure 3;  $\mathcal{P}$  is defined in equation (15), and  $r$  is dimensionless.

that, for  $l = 3$  (and probably for  $l = 4$  also), the eigenvalue is continuous as  $R_c \rightarrow 0$  with the  $E_3$  (and  $E_4$ ) of the coreless model, results for which are shown on the  $E$  axis. In sharp contrast,  $E_2$  displays a number of ‘spikes’ resembling asymptotes.

From the mathematical standpoint, the sensitivity of  $E_2$  to  $R_c$  shown in figure 8 may be partially understood by observing that, when  $R_c$  and  $r (> R_c)$  are sufficiently small,

$$R \sim A_l r \sin \left[ s \ln \left( \frac{r}{R_c} \right) \right] + B_l r^{5/4} \cos \left[ \frac{4}{\sigma} \left( \frac{1}{r^{1/2}} - \frac{1}{R_c^{1/2}} \right) \right], \quad (16)$$

where  $A_l$  and  $B_l$  are constants whose ratio is determined by conditions at  $r = \infty$ . It appears that, for any  $\sigma$  and sufficiently large  $l$ , the ratio  $B_l/A_l \rightarrow 0$  as  $R_c \rightarrow 0$ , and the solution (16) for the hard core is continuous with that of the coreless model (which



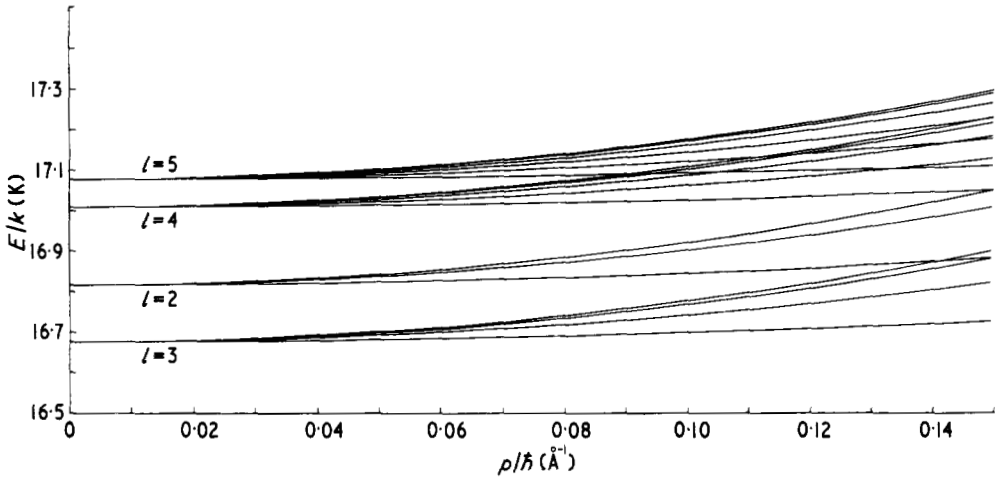


**Figure 6.** The computed dispersion curves (1) for the bound states  $l = 2, 3, 4$  and  $5$  ( $0 \leq m \leq l$ ) on the assumption of a pure dipole-dipole interaction.

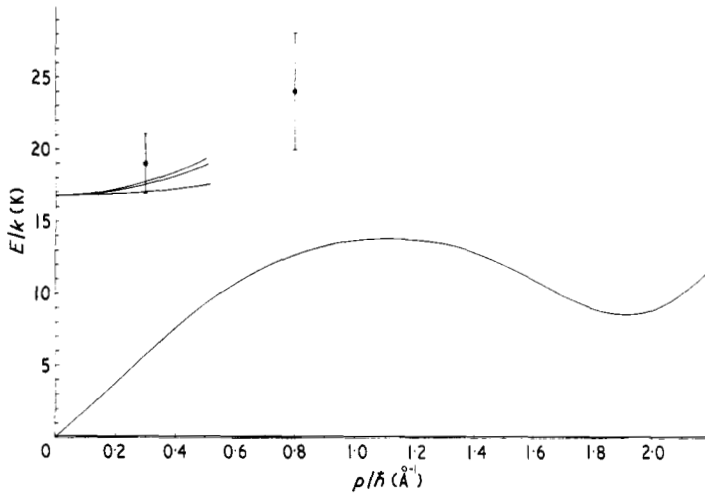


**Figure 7.** The computed dispersion curve (1) for the the bounds states  $l = 2$  ( $m = 0, 1, 2$ ) on the assumption of a pure dipole-dipole interaction. Also shown are a model dispersion curve for unbound excitations, and neutron data.

contains no irregular component). It also appears that, for any  $l$  and sufficiently small  $\sigma$ , the ratio  $B_l/A_l$  for the maximally bound state(s) is  $O(1)$  as  $R_c \rightarrow 0$ , leading to the irregular behaviour evident for  $l = 2$  in figure 8. Further support for this view is shown in table 2. It may be seen that, if the dipole interaction is sufficiently weakened (larger  $\sigma$ ),  $E_2$  is a smooth function of  $R_c$ . When it is strengthened (small  $\sigma$ ), even  $E_3$  is no longer a smooth function of  $R_c$ . It is doubtful whether the soft-core solutions are continuous with the bumpy hard-core solutions but it is possible that they are continuous with a less tightly bound, but smooth, branch of the hard-core solutions: we obtained no numerical evidence of this.

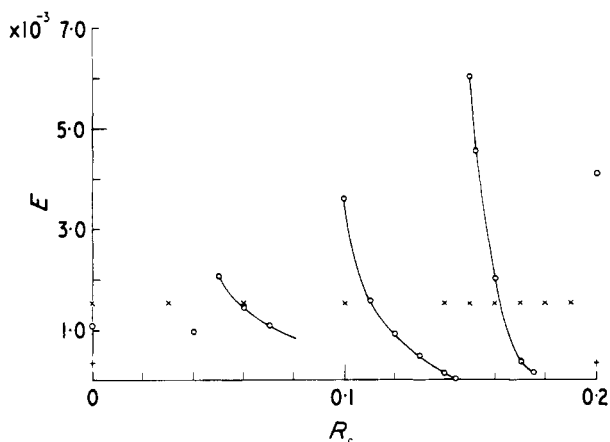


**Figure 8.** The binding energy  $E$  as a function of hard-core radius  $R_c$  for  $l = 2, 3$  and  $4$ . The open circles give the computed values of the most tightly bound states for  $l = 2$ , the crosses for  $l = 3$ , and the plus signs for  $l = 4$ .

**Table 2.** Some binding energies of the hard core model.

		$\sigma = 1$				
$R_c$		0	0.10	0.16	0.20	
$10^5 E_2$		5.803	5.790	5.777	5.772	
		$\sigma = 0.2$				
$R_c$		0	0.145	0.15	0.165	0.17
$10^5 E_3$		48.21	8.415	2.076	36.79	16.79
						6.867

$R_c$  in units of  $\lambda$ , and  $E_l$  in units of  $p_0^2/\mu$ .

From the physical standpoint, the sensitivity of  $E_2$  to  $R_c$  shown in figure 8 is reminiscent of the falling of a particle into a sufficiently strong centre of attraction (Landau and Lifshitz 1958, § 25), and it is perhaps significant that the classical theory of roton binding (Roberts and Donnelly 1973, 1974) predicts that falling in must occur for all sufficiently small angular momenta, more precisely whenever

$$\sigma[l(l+1)]^{1/2} < 1.6865 \dots \tag{17}$$

Moreover, the value of 0.499 used for  $\sigma$  in preparing figure 8 lies between the two critical values, 0.689 and 0.487, given by (17) for  $l = 2$  and 3 respectively. On the other hand, the values of  $\sigma$  used in table 2 lie outside this interval.

It appears from this discussion that results obtained for fixed  $\sigma$  and sufficiently large  $l$  will be insensitive to the short-range deviations from the dipole-dipole interaction which probably arise between rotors. We may also anticipate that, if the short-range potential is sufficiently smooth compared with the (varying) oscillation period of the irregular solutions, the sensitivity of  $E_l$  to  $R_c$  for fixed  $l$  and sufficiently small  $\sigma$  will be removed. In the absence of any firm knowledge about the interaction potential at short distances, we have, however, not deemed it profitable to continue the calculations by adding to the dipole law in an *ad hoc* way.

Although we did not examine the soft-core model in detail, its behaviour appears to resemble that of the hard-core model. We note that Yau and Stephen (1971), after performing variationally a calculation somewhat similar to ours, reported that the binding energy  $E_2$  is sensitive to  $R_c$ , with experiment best fitted when  $R_c \approx 5 \text{ \AA}$ .

We feel that our theoretical results, taken in conjunction with the experimental data, provide convincing evidence for the existence of bound states, and that these states are likely to provide a good basis for further theoretical and experimental elucidation of the He II excitation spectrum. We also feel that experimentalists may wish to be made aware of the theoretical possibility that the optically observed  $l = 2$  states may not be statistically the most numerous.

### Acknowledgments

We would like to record our indebtedness to Professor Russell J Donnelly for encouraging us to examine the problem considered here, for his keen interest in our work, for his criticism of the first version of our paper, and for his hospitality at the University of Oregon. John C Nosler introduced us to the operating procedures of the Hewlett-Packard computer on which some of the working programs were developed, and Subodh Kumar kindly undertook the entire production work on the IBM 360-67 at the University of Newcastle. Some helpful remarks by a referee are acknowledged. The research was supported by NSF GH-35898 and AF-AFOSR-71-1999.

### References

- Brooks J and Donnelly R J 1974 *J. Low Temp. Phys.* to be published  
 Cowley R A and Woods A D B 1971 *Can. J. Phys.* **49** 177  
 Donnelly R J 1972 *Phys. Lett.* **39A** 221  
 Feenberg E 1969 *Theory of Quantum Fluids* (New York and London: Academic Press)  
 Feynman R P and Cohen M 1956 *Phys. Rev.* **102** 1189  
 Greytak T J, Woerner R, Yau J and Benjamin R 1970 *Phys. Rev. Lett.* **25** 1547  
 Greytak T J and Yau J 1969 *Phys. Rev. Lett.* **22** 987  
 Iguichi I 1971 *J. Low Temp. Phys.* **4** 637  
 Landau L D and Lifshitz E M 1958 *Quantum Mechanics: Non-Relativistic Theory* (London and Paris: Pergamon Press)  
 Roberts P H and Donnelly R J 1973 *Phys. Lett* **43A** 1  
 ——— 1974 *J. Low Temp. Phys.* **15** 1  
 Yau J and Stephen M J 1971 *Phys. Rev. Lett.* **27** 482